16 April 1999

ELSEVIER

Chemical Physics Letters 303 (1999) 531–536

CHEMICAL PHYSICS LETTERS

Generalized reaction–diffusion equations

G.W. Wei *

Department of Computational Science, National University of Singapore, Singapore 119260, Singapore

Received 18 December 1998; in final form 28 January 1999

Abstract

This Letter proposes generalized reaction–diffusion equations for treating noisy magnetic resonance images. An edge-enhancing functional is introduced for image enhancement. A number of super-diffusion operators are introduced for fast and effective smoothing. Statistical information is utilized for robust edge-stopping and diffusion-rate estimation. A quasi-interpolating wavelet algorithm is utilized for numerical computations. Computer experiments indicate that the present algorithm is efficient for edge detecting and noise removing. The generalized reaction–diffusion equations have potential applications in modeling boundary-restricted diffusion, multiphase chemical reactions and reaction–diffusion in porous media.

It is well known that the evolution of an image under certain partial differential equation (PDE) operators is an image processing operation [1–3]. Correspondingly, an image processing operation, under appropriate restrictions, can be regarded as action of a PDE operator [4]. This link between PDEs and image processing has stimulated much interest in both fields. The use of (linear) PDE operators in image processing began with the diffusion operator and has its roots in the theory of multiscale analysis and Gaussian smoothing initiated by Rosenfeld and Thurston [1] and others [2,3]. It can be proved that the heat equation satisfies the maximum and minimum principles, which means the maximum and minimum can only be attained for the initial image data or at the boundary of an image [5]. Hence, the edges of an image may lose definition under the action of the diffusion operator.

Perona and Malik [6] addressed the edge loss problem by introducing a (non-linear) anisotropic diffusion operator [6]. Such a formalism has stimulated a great deal of interest [7–20]. It is commonly believed that the Perona–Malik algorithm provides a potential means for noise removing, edge detection, image segmentation and enhancement. The basic idea behind the Perona–Malik algorithm is to regard an original image $I(\boldsymbol{r})$ as evolving under an edge-stopping diffusion operator

$$\frac{\partial u(\boldsymbol{r},t)}{\partial t} = \boldsymbol{\nabla}\cdot\left[d(|\nabla u(\boldsymbol{r},t)|)\nabla u(\boldsymbol{r},t)\right],$$

$$u(\boldsymbol{r},0) = I(\boldsymbol{r}), \qquad (1)$$

where $d(|\nabla u|)$ is a generalized diffusion coefficient which is so designed that it limits the diffusion near edges while allowing lots of diffusion in regions where the noise is to be suppressed. The edges of an

* Corresponding author. Fax: +65 774 6756; e-mail: cscweigw@nus.edu.sg

0009-2614/99/$ - see front matter
PII: S0009-2614(99)00270-5

image are automatically detected by using a diffusion rate based on approximating the norm of the gradient across edges with the norm of the full image gradient. Examples of such coefficients, as suggested originally by Perona and Malik, include

$$d(|\nabla u|) = \exp\left[-\frac{|\nabla u|^2}{2\eta^2}\right], \tag{2}$$

and

$$d(|\nabla u|) = \frac{1}{1+\dfrac{|\nabla u|^2}{\eta^2}}, \tag{3}$$

where η is a threshold value. It is well-known [7,9,11,13] that this anisotropic diffusion algorithm may break down when the gradient generated by noise is comparable to image edges and features. In mathematical terms, the Perona–Malik equation (Eq. (1)) is ill defined. This problem may be alleviated through a regularizer $R(\boldsymbol{r})$ which serves both as a low-pass filter for removing high-frequency noise and as a smoother for the possible discontinuity in the original image function

$$\frac{\partial u(\boldsymbol{r},t)}{\partial t} = \boldsymbol{\nabla}\cdot\left\{d\left[|\nabla(R(\boldsymbol{r}) * u(\boldsymbol{r},t))|\right]\nabla u(\boldsymbol{r},t)\right\}, \tag{4}$$

where $R(\boldsymbol{r}) * u(\boldsymbol{r},t)$ denotes the convolution. Possible choices of regularizers are Gaussian [7], Lorentzian function $(1/\pi)[\alpha/(\alpha^2+x^2)]$, and Shannon's scaling function $\sin(\alpha x)/(\pi x)$. Mathematically, this scheme provides a weak solution of the original Perona–Malik equation.

The purpose of this Letter is to introduce generalized reaction–diffusion equations for treating noisy images. Such equations can be derived from conservation laws and can be regarded as generalizations of the Perona–Malik equation (Eq. (1)). Statistical information is used for automatic edge-stopping and noise-level estimation. A time-dependent threshold is introduced to handle possible break down due to a noise-generated gradient. A recently developed quasi-interpolating wavelet algorithm [21] is utilized for the numerical integration of generalized reaction–diffusion equations. The efficiency and robustness of the present algorithm are illustrated by its application to magnetic resonance images (MRI).

In many physical situations, the edges of an image may be degraded for various reasons. In other cases, the resolution of an image can be very low; for example, X-ray breast mammogram images, where the difference in X-ray attenuation between normal and cancerous tissues is very small. Similar cases can appear in MRIs. Therefore, a direct feature enhancement is often required. We propose a real-valued *edge-enhancing functional*

$$e\left[u(\boldsymbol{r},t),|\nabla u(\boldsymbol{r},t)|\right], \tag{5}$$

where $|e|<\infty$ is bounded up and below. It is appropriately chosen so that a certain image feature and/or the contrast of image edges are enhanced during the time propagation. This leads to a generalized reaction–diffusion equation

$$\frac{\partial u(\boldsymbol{r},t)}{\partial t} = \boldsymbol{\nabla}\cdot\left\{d\left[u(\boldsymbol{r},t),|\nabla u(\boldsymbol{r},t)|\right]\nabla u(\boldsymbol{r},t)\right\} + e\left[u(\boldsymbol{r},t),|\nabla u(\boldsymbol{r},t)|\right],$$
$$u(\boldsymbol{r},0) = I(\boldsymbol{r}). \tag{6}$$

For constant d and a simple form of e, Eq. (6) reduces to the inhomogeneous diffusion equation. The maximum and minimum principles are important for proving uniqueness and continuous dependence on the initial data for the solution of initial and boundary value problems for the diffusion equation. A strong maximum or minimum principle is known for the inhomogeneous diffusion equation and a weak maximum or minimum principle is known for the homogeneous diffusion equation [5]. Perona–Malik argued that their anisotropic diffusion equation has no additional maxima (minima) which do not belong to the initial image data. Since the source term in the generalized reaction–diffusion equation (Eq. (6)) is effectively non-zero only at image edges or at a feature, it retains the strong maximum or minimum principle and thus preserves image features.

The derivation of the diffusion equation (heat equation) is based on Fourier's law for heat flux

$$\boldsymbol{j}_1(\boldsymbol{r},t) = -D_1\nabla u(\boldsymbol{r},t). \tag{7}$$

Here D_1 is a constant. This, from the point of view of kinetic theory, is a simplified approximation to a quasi-homogeneous system which is near equilib-

rium. A better approximation can be expressed as a super flux term

$$\boldsymbol{j}_q(\boldsymbol{r},t) = -\sum_q D_q \nabla \nabla^{2q} u(\boldsymbol{r},t)\,, \tag{8}$$

where D_q are constants and high order terms ($q>1$) describe the influence of inhomogeneity in temperature field and flux–flux correlations. Energy conservation leads to

$$\frac{\partial u(\boldsymbol{r},t)}{\partial t} = -\nabla\cdot\boldsymbol{j}_q(\boldsymbol{r},t) + s(\boldsymbol{r},t) = \sum_q \nabla\cdot\left[D_q \nabla\nabla^{2q} u(\boldsymbol{r},t)\right] + s(\boldsymbol{r},t)\,, \tag{9}$$

where s is a productive (source) term which can be a non-linear function describing chemical reactions. Eq. (9) is an interesting reaction–diffusion equation which includes not only the usual diffusion and production terms, but also a 'super'-diffusion term. The case of second-order super-diffusion, $\boldsymbol{j}_2(\boldsymbol{r},t) = -D_1\nabla u(\boldsymbol{r},t) + |D_2|\nabla\nabla^2 u(\boldsymbol{r},t)$, has been used for the decription of a number of physical phenomena, such as pattern formation in alloys, glasses, polymer, combustion and biological systems.

In image systems, the distribution of image pixels can be highly inhomogeneous. Hence, the generalized reaction–diffusion equation (Eq. (6)) can be made more efficient for image segmentation and noise removing by incorporating an edge-sensitive super-diffusion term

$$\frac{\partial u(\boldsymbol{r},t)}{\partial t} = \sum_q \boldsymbol{\nabla}\cdot\left\{d_q\left[u(\boldsymbol{r},t),|\nabla u(\boldsymbol{r},t)|\right] \times\nabla\nabla^{2q}u(\boldsymbol{r},t)\right\} + e\left[u(\boldsymbol{r},t),|\nabla u(\boldsymbol{r},t)|\right]. \tag{10}$$

Here $d_q(u,|\nabla u|)$ are edge-sensitive diffusion functions. Eq. (10) is a generalized reaction–diffusion equation and it can also be regarded as a generalization of the Perona–Malik equation (Eq. (1)). A special form used in this Letter for numerical experiments is

$$\frac{\partial u(\boldsymbol{r},t)}{\partial t} = \boldsymbol{\nabla}\cdot\left\{d_1\left[u(\boldsymbol{r},t),|\nabla u(\boldsymbol{r},t)|\right]\nabla u(\boldsymbol{r},t)\right\} + \boldsymbol{\nabla}\cdot\left\{d_2\left[u(\boldsymbol{r},t),|\nabla u(\boldsymbol{r},t)|\right]\nabla\nabla^2 \times u(\boldsymbol{r},t)\right\} + e\left[u(\boldsymbol{r},t),|\nabla u(\boldsymbol{r},t)|\right]. \tag{11}$$

The diffusion functions can be appropriately chosen in many different ways. In this Letter, we choose the Gaussian, for both $d_1(u,|\nabla u|)$ and $d_2(u,|\nabla u|)$

$$d_q(u,|\nabla u|) = d_{q0}\exp\left[-\frac{|\nabla u|^2 t}{2\sigma_1^2 t_0}\right], \tag{12}$$

where d_{q0} are automatically determined by the noise level σ_0 and t_0 is a *time delay* value at which the edge-stopping becomes more important. Here σ_0 and σ_1 are chosen as local statistical variances of u and ∇u

$$\sigma_q^2(\boldsymbol{r},t) = \overline{|\nabla^q u - \overline{\nabla^q u}|^2}, \quad (q=0,1). \tag{13}$$

Here $\overline{X(\boldsymbol{r})}$ denotes the local average of $X(\boldsymbol{r})$ centered at point $\boldsymbol{r}$. The area of local average used in this Letter is 17×17 pixel^2. Obviously, these local statistical variances can be optimized for a given problem. However, we have not implemented this optimization in this work. The appropriate use of time delay t_0 can effectively prevent the noise-break down of the original Perona–Malik equation. Certainly, this concept can be implemented in a variety of ways. In this work, we choose the edge enhancing functional as

$$e(u,|\nabla u|) = e_0(u)\frac{|\nabla u|^2}{\sigma_1^2}\mathrm{e}^{-[(t-t_e)^2]/(2\sigma_e^2)}, \tag{14}$$

with $e_0(u)$ varying as a function of u. Here, $\mathrm{e}^{-[(t-t_e)^2]/(2\sigma_e^2)}$ is designed to turn on the edge-enhancing functional for an effective period of the size of σ_e centered at t_0.

The Perona–Malik equation (Eq. (1)) and generalized reaction–diffusion equations (Eqs. (6) and (11)) are spatially discretized using a quasi-interpolating wavelet algorithm [21]

$$\frac{\partial^l u(x,y)}{\partial x^m \partial y^{l-m}} \approx \sum_{k=-W_x}^{W_x}\sum_{j=-W_y}^{W_y} \overline{\Phi}^{(m)}_{\sigma_x,\Delta_x}(x-x_k) \times \overline{\Phi}^{(l-m)}_{\sigma_y,\Delta_y}(y-y_j)\,u(x_k,y_j)\,, \tag{15}$$

where $\overline{\Phi}^{(m)}_{\sigma_y,\Delta_y}(x-x_k)$ is the mth derivative of the quasi-interpolating wavelet scaling function [21]. Here, $\sigma_x/\Delta_x = \sigma_y/\Delta_y = 3.2$ and $W_x = W_y = 8$ are used to discretize the variable of the diffusion coefficients for removing noise and accurately detecting edges. Our quasi-interpolating wavelet algorithm is a discrete singular convolution method which provides a weak solution to a partial differential equation. The additional regularization operation as indicated in Eq. (4) is no longer necessary in our approach. The fourth-order Runge–Kutta method is employed for the time discretization of the Perona–Malik equation and its generalizations. A reflecting boundary condition is used in time integration.

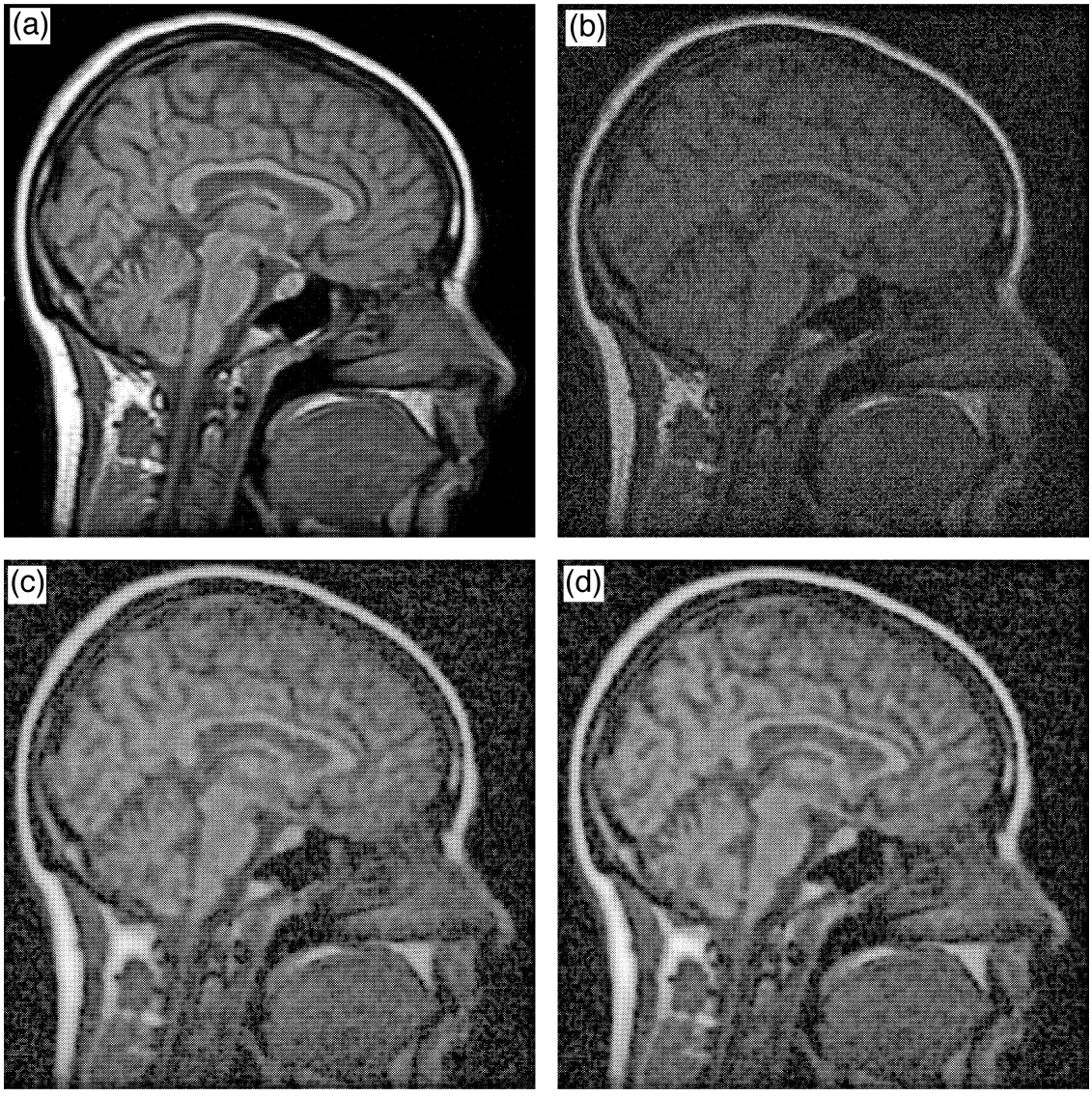

Fig. 1. Restoration of a noisy magnetic resonance image. (a) Original image; (b) noisy image; (c) restored with the Perona–Malik diffusion operator; (d) restored with the Perona–Malik diffusion operator and the edge-enhancing functional; (e) restored with the Perona–Malik diffusion operator, the super-diffusion operator and the edge-enhancing functional.

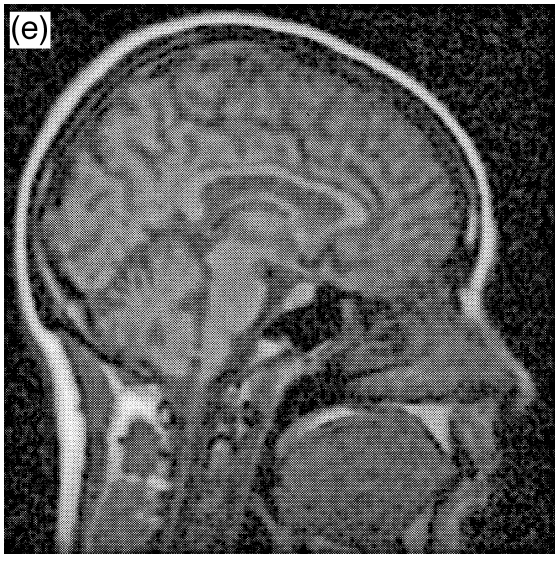

Fig. 1 (continued).

We use a 256×256 MRI sample (Fig. 1a) for our demonstration. The MRI sample is degraded with Gaussian noise to obtain a peak signal-to-noise ratio (PSNR) of 25 dB (Fig. 1b). The PSNR used here is calculated as

$$\mathrm{PSNR} = \frac{255 \times 255}{\frac{1}{N_x N_y} \sum_{i=1}^{N_x} \sum_{j=1}^{N_y} \left[I_0(i,j) - u(i,j) \right]^2}, \quad (16)$$

where $I_0(i,j)$ and $u(i,j)$ are the original image, which is assumed to be noise free, and noisy image samples, respectively, and N_x and N_y are the number of pixels horizontally and vertically, respectively. The parameters t_0, t_e, d_{10}, d_{20}, and $e_0(u)$ are chosen as 18, 3.5, $0.4\sigma_0$, $-0.006\sigma_0$ and $-0.01u$ respectively. Fig. 1c shows the restored MRI produced by using the Perona–Malik equation (Eq. (1)). The increase in PSNR is quite large (20 dB) with the use of the autothreshold technique and the quasi-interpolating wavelet algorithm. Fig. 1d is obtained by the combined use of the edge-enhancing functional and the Perona–Malik anisotropic diffusion operator (Eq. (6)). Obviously, the edge of the image is effectively enhanced by the edge-enhancing functional as indicated by an increase of PSNR of 29 dB. The performance of the full generalized Perona–Malik equation (Eq. (11)) is given in Fig. 1e. In this case, the PSNR is increased by 35 dB. Comparing them with the degraded image (Fig. 1b), it is clearly seen that the present algorithms can effectively remove noise while simultaneously preserving the edges. The image boundary is also effectively preserved, which shows the success of the present reflecting boundary treatment. As pointed out in Ref. [14], for noisier images the Perona–Malik equation may produce some noise echoes that are larger than the threshold value and thus cannot be removed. However, increasing the threshold value leads to edge-blurring. Using the various techniques presented in this Letter and in Ref. [21], we can effectively avoid the problem by accurately detecting the edges using the quasi-orthogonal wavelets. Since our quasi-interpolating wavelets are functions of the Schwartz class, the present algorithm of time integration automatically avoids having to apply an additional smoothing operation to the argument of the diffusion coefficient. We have also tested our algorithm for even nosier images and have found that it can increase the PSNR enormously.

In conclusion, we propose generalized reaction–diffusion equations for edge-detected image processing. An edge-enhancing functional is introduced for direct image enhancement. Such a term is very useful for enhancing low contrast images and edge-blurred images. We also introduce edge-detected super-diffusion operators for highly inhomogeneous images. The super-diffusion operators are very efficient for noise-removing. Statistical information is used for the automatical choice of edge-stopping threshold and for determining diffusion amplitudes. A time delay concept is used in edge-stopping coefficients for preventing high noise-level breakdown. A newly developed quasi-interpolating wavelet technique [21] is used for the time integration of the PDE system. Numerical experiments on a noisy MRI sample show that the present algorithm is very effective for noise-removing and simultaneously edge-preserving. While the application addressed in this work is MRI restoration, we note that the present generalized reaction–diffusion equations have great potential for theoretical modeling of various physical phenomena, such as boundary-restricted diffusion, multiphase chemical reaction and reaction–diffusion in porous media. These aspects are under investigation.

Acknowledgements

This work was supported in part by the National University of Singapore. The author thanks Drs. E.C. Chang and Y.P. Wang, and Prof. Yingfei Yi for useful discussions.

References

[1] A. Rosenfeld, M. Thurston, IEEE Trans. Comp. C 20 (1971) 562.
[2] D.H. Ballard, C.M. Brown, Computer Vision, Prentice Hall, Englewood Cliffs, NJ, 1982.
[3] D. Marr, T. Poggio, Proc. R. Soc. Lond. B 204 (1979) 301.
[4] L. Alvarez, F. Guichard, P. Lions, J. Morel, Centre de Recherche de Mathematiques de la Decision, Number 9254, November 1992.
[5] E. Zauderer, Partial Differential Equations of Applied mathematics, Wiley, New York, 1989.
[6] P. Perona, J. Malik, IEEE Trans. Pattern Anal. Machine Intell. 12 (1990) 629.
[7] F. Catte, P.-L Lions, J.-M. Morel, T. Coll, SIAM J. Numer. Anal. 29 (1992) 182.
[8] L. Alvarez, P.-L Lions, J.-M. Morel, SIAM J. Numer. Anal. 29 (1992) 845.
[9] M. Nitzberg, T. Shiota, IEEE Trans. Pattern Anal. Machine Intell. 14 (1992) 826.
[10] L. Rudin, S. Osher, E. Fatemi, Physica D 60 (1992) 259.
[11] R.T. Whitaker, S.M. Pizer, CVGIP: Image Understanding 57 (1993) 99.
[12] Y.-L You, M. Kaveh, W.-Y Xu, T. Tannenbaum, in IEEE Proc. 1st Int. Conf. Image Processing, Austin, TX, November, vol. II, 1994, p. 497.
[13] Y.-L. You, W. Xu, A. Tannenbaum, M. Kaveh, IEEE Trans. Image Process. 5 (1996) 1539.
[14] F. Torkamani-Azar, K.E. Tait, IEEE Trans. Image Process. 5 (1996) 1573.
[15] G. Sapiro, in: IEEE Proc. 3rd Int. Conf. Image Processing, Lausanne, Switzerland, vol. I, 1996, p. 477.
[16] J. Shah, in: IEEE Proc. Conf. Computer Vision and Pattern Recognition, San Francisco, CA, 1996, p. 136.
[17] S.T. Acton, in: IEEE Proc. 3rd Int. Conf. Image Processing, Lausnne, Switzerland, 1996, p. 865.
[18] E. Bänsch, K. Mikula, Comput. Visual Sci. 1 (1997) 53.
[19] S. Teboul, L. Blanc-Feraud, G. Aubert, M. Barlaud, IEEE Trans. Image Process. 7 (1998) 387.
[20] M.J. Black, G. Sapiro, D.H. Marimont, D. Heeger, IEEE Trans. Image Process. 7 (1998) 421.
[21] G.W. Wei, Chem. Phys. Lett. 296 (1998) 215.